

# Circular discrepancy and a Monte Carlo algorithm for generating a low circular discrepancy sequence

By

Syed M. Assad, Physics Department, National University of Singapore

and

Chjan C. Lim, Mathematical Sciences, Rensselaer Polytechnic Institute

Troy, NY 12180, USA

+

## Abstract

We present a numerical method for generating a low discrepancy point sequence inside the circle. The method is based on physically minimizing the energy of a vortex gas system and naturally incorporates the random fluctuations in a simulated system at positive temperatures. The quality of this distribution of points is compared against two sequences obtained from the Hammersley sequence and the Sobol sequence, using the half-plane notion of discrepancy also known as circular discrepancy.

## 1 Introduction

This paper deals with discrepancy of  $N$  points in the disc and a new method for generating low discrepancy sequences. Numerous algorithm [9] have been developed for generating low discrepancy points on the cube  $I^s = [0, 1]^s$ . On the cube, low discrepancy points are of importance in performing quasi Monte-Carlo methods. For example to numerically evaluate the proper integral of a function of bounded variation  $f(\vec{x})$ , we can estimate this integral of  $f$  by sampling  $f$  at  $N$  points. Then Koksma's inequality bounds the integration error by  $V(f)D_N^*$ , where  $V(f)$  reflects the regularity of  $f$  and  $D_N^*$  describes the regularity (discrepancy) of the points [6, 8].

Consider the simple problem of approximating the area of a disc segment (an intersection of a disc with a half plane) by choosing  $N$  random points in the disc, and counting the number of points that falls in this disc segment. The area of the segment can then be approximated by  $x/N$ , where  $x$  is the number of points falling in the disc segment. As  $N$  gets larger, we expect

that the approximation would get better. It is well known that the error of this random or Monte Carlo method is  $O(N^{-1/2})$ .

Quasi Monte Carlo methods on the other hand use deterministic sequences of points to perform the numerical integration of sufficiently smooth functions. In principle the integration error of these methods is  $O(N^{-1}(\log N)^d)$  where  $d$  is the dimension of the domain of integration. There is evidence that the quasi Monte Carlo methods outperform the traditional Monte Carlo methods when the effective dimension of the integrands are not too high (see Morokoff and Caffisch [6] and Owen [10] for a definition of the effective dimension of a large class of integrands).

Hybrid Monte Carlo quasi Monte Carlo methods where the integration mesh from a quasi MC method has been perturbed by random fluctuations, are known to have better asymptotic error of  $O(N^{-3/2}(\log N)^d)$  (see [10]). Our method is based on the equilibrium statistical mechanics of point vortex logarithmic interactions and naturally incorporates the random fluctuations of a simulated system at positive temperatures.

This paper is organized as follows. In section 2, we shall define the circular discrepancy of  $N$  points in a disc. This is defined as the maximum possible error in approximating the area of an arbitrary disc segment given  $N$  fixed points. This shall be used to quantify the quality of a sequence of points in the disc.

We show in section 3 that given an arbitrary sequence of  $N$  points, its circular discrepancy can be measured in  $O(N^3)$  time. Section 4 presents a method for generating  $N$  well distributed points in the disc that achieves a low circular discrepancy. This method is based on Monte-Carlo simulations of a vortex gas system.

In section 5 we introduce the square discrepancy. Square discrepancy measures the ‘uniformity’ of a sequence of points on the square. We shall use two quasi-random sequences with low square discrepancy, namely the Hammersley sequence and the Sobol sequence to provide numerical comparisons with the vortex gas sequence.

Finally sections 6.2 and 6.3 presents the numerical results.

## 2 Circular discrepancy

*Definition:* Let  $\mathcal{P}$  be an arbitrary distribution of  $N$  points in the circular disc  $D$  of unit area. For each disc segment  $A$  (i.e. an intersection of  $D$  with a half-plane), let  $Z[\mathcal{P}; A]$  denote the

number of elements of  $\mathcal{P}$  which lies in  $A$ . We define the circular discrepancy of  $\mathcal{P}$  with respect to  $A$  as

$$\Delta[\mathcal{P}; A] = \left| \frac{Z[\mathcal{P}; A]}{N} - \mu(A) \right|$$

where  $\mu(A)$  denotes the usual area of  $A$ . The circular discrepancy of  $\mathcal{P}$  is then defined as

$$\Delta[\mathcal{P}] = \sup_A \Delta[\mathcal{P}; A]$$

where the supremum is taken over all disc segments  $A$  of  $D$ . Finally the best discrepancy (for  $N$  points) is defined by

$$\Delta[N] = \inf_{\mathcal{P}} \Delta[\mathcal{P}]$$

$\Delta[N]$  is bounded as follows [3]:

$$c_1 N^{-\frac{3}{4}} (\log N)^{-\frac{7}{2}} < \Delta[N] < c_2 N^{-\frac{3}{4}} (\log N)^{\frac{1}{2}},$$

where  $c_1$  and  $c_2$  are constants.

### 3 Measuring $\Delta[\mathcal{P}]$

In this section, we shall show that given a distribution of  $N$  points  $\mathcal{P}$ , its circular discrepancy  $\Delta[\mathcal{P}]$  can be measured in polynomial  $N$  time.

We can replace the infinite set of half-plane  $A$  in the supremum with a finite subset without affecting the value of  $\Delta[\mathcal{P}]$ . We first identify a finite set of half-planes that would have maximum local discrepancy as follows: If lets say the edge of the half-plane  $A$  does not contain a point  $p \in \mathcal{P}$ , then unless this edge is a diameter, it can be translated slightly to make  $\mu(A)$  bigger. This edge can also be translated in the opposite direction to make  $\mu(A)$  smaller. As long as either of these two translations is small enough so that it does not cross any points in  $\mathcal{P}$ , the counting function  $Z[\mathcal{P}; A]$  does not change. So one of the two translation results in an increase in circular-discrepancy  $\Delta[\mathcal{P}; A]$ .

If the edge of the half-plane  $A$  is a diameter of  $D$ , then we can rotate this edge about the center of  $D$  without affecting the value of  $\mu(A)$ . If the rotation is small such that it does not cross any points in  $\mathcal{P}$ , then the counting function  $Z[\mathcal{P}; A]$  does not change. Hence all this

family of rotated half-planes would have the same circular-discrepancy  $\Delta[\mathcal{P}; A]$  with a particular half-plane that has a point  $p \in \mathcal{P}$  on its edge.

Hence the half-plane we are looking for in maximizing the circular-discrepancy  $\Delta[\mathcal{P}; A]$  has a point of  $p$  on its boundary. Thus

**Theorem 3.1** *Let  $\mathcal{P}$  be a set of  $N$  points in the circular disc  $D$  of unit area. The disc segment  $A$  that achieves the maximum discrepancy with respect to  $\mathcal{P}$  is one of the following types:*

- (i) *A contains one point  $p \in \mathcal{P}$  on its boundary,*
- (ii) *A contains two or more points of  $\mathcal{P}$  on its boundary.*

**Theorem 3.2** *For type (i), the disc segment  $A$  that contains one point  $p_i \in \mathcal{P}$  locally extremize  $\mu(h)$  when the boundary of  $A$  is perpendicular to the line that contains  $p_i$  and the center of the disk. See figure 1(a).*

Proof: Let  $p$  be a point in  $\mathcal{P}$ . Without loss of generality, we can set up our coordinate axis such that  $p$  lies on the positive  $y$ -axis, with coordinates  $(p_x, p_y) = (0, y)$ . Consider the disc segment  $A_p(\phi)$ , whose boundary  $l(\phi)$  contains  $p$  and makes the angle  $\phi$  with the positive  $y$ -axis. The disc segment contains all point directly above  $p$  when  $0 < \phi < \pi$ , and it contains all points below  $p$  when  $\pi < \phi < 2\pi$ .

When  $0 < \phi < \pi$ , the area of  $A_p(\phi)$  is:

$$\mu(A_p(\phi)) = R^2 \cos^{-1} \left( \frac{d_1}{R} \right) - d_1 \sqrt{R^2 - d_1^2},$$

where  $R$  is the radius of  $D$  and  $d_1 = y \sin \phi$  is the closest distance between  $l(\phi)$  and the center of  $D$ .

When  $\pi < \phi < 2\pi$ , the area of  $A_p(\phi)$  is:

$$\begin{aligned} \mu(A_p(\phi)) &= \pi R^2 - \mu(A_p(\phi - \pi)) \\ &= \pi R^2 - \left( R^2 \cos^{-1} \left( \frac{d_2}{R} \right) - d_2 \sqrt{R^2 - d_2^2} \right), \end{aligned}$$

where  $d_2 = y \sin(\phi - \pi) = -y \sin \phi$  is the closest distance between  $l(\phi)$  and the center of  $D$ .

We want to find the value of  $\phi^*$  which would locally extremizes  $\mu(A_p(\phi))$ . Scaling the unit disc  $D$  to the disc of unit radius would not change the value of  $\phi^*$ . Hence setting  $R = 1$ , we get

$$\mu(A_p(\phi)) = \begin{cases} \cos^{-1}(y \sin \phi) - y \sin \phi \sqrt{1 - y^2 \sin^2 \phi} & , \text{ if } 0 \leq \phi < \pi \\ \pi - \cos^{-1}(-y \sin \phi) - y \sin \phi \sqrt{1 - y^2 \sin^2 \phi} & , \text{ if } \pi \leq \phi < 2\pi \end{cases}$$

$\mu(A_p(\phi))$  as parameterized by  $\phi$  is continuous and smooth since it represents the area of the disc segment  $A_p(\phi)$ . To find the local extremas of  $\mu(A_p(\phi))$ , we differentiate  $\mu(A_p(\phi))$  with respect to  $\phi$ .

$$\begin{aligned} \frac{d\mu(A_p(\phi))}{d\phi} &= -\frac{y \cos \phi}{\sqrt{1 - y^2(\sin \phi)^2}} + \frac{y^3 \cos \phi (\sin \phi)^2}{\sqrt{1 - y^2(\sin \phi)^2}} - y \cos \phi \sqrt{1 - y^2(\sin \phi)^2} \\ &= -y \cos \phi \sqrt{4 - 2y^2 + 2y^2 \cos(2\phi)} \end{aligned}$$

Setting  $d\mu(A_p(\phi))/d\phi$  to zero, we get two real solutions,  $\phi = \pi/2$  and  $\phi = 3\pi/2$ . •

Having identified the disc segments  $A$  that achieves maximum local discrepancy for type (i), now we can proceed to calculate this discrepancy,  $\Delta[\mathcal{P}; A]$ .

**Remark 3.1** Let  $p_i = (x_i, y_i)$  be an arbitrary point in  $\mathcal{P}$ . If  $p_i$  lies on the center of the disc, then the disc segment of type (i) is not uniquely defined. However, all this family of disc segment have the same area, and one could rotate the disc segment such that they contain two points of  $\mathcal{P}$ . Then these disc segments could be dealt with as type (ii).

If  $p_i$  is not exactly on the center, then the disc segment  $A$  of type (i) that achieves maximum local discrepancy would have its boundary on the line  $l(x_i, y_i)$ , where  $l$  passes through  $p_i$  with slope  $-x_i/y_i$ . Two disc segments share this boundary. Let  $A_1$  be the disc segment with smaller area. We count  $Z[\mathcal{P}; A_1]$  as follows: if  $y_i \geq 0$ , then  $Z[\mathcal{P}; A_1] = \sum_{j \neq i}^N g(p_j)$ , where

$$g(p_j) = \begin{cases} 1 & , \text{ if } p_j \text{ lies above } l(x_i, y_i) \\ 0 & , \text{ otherwise.} \end{cases}$$

If  $y_i < 0$ , then  $Z[\mathcal{P}; A_1] = \sum_{j \neq i}^N (1 - g(p_j))$ .

The possible candidates for the discrepancy would then be:

$$\left\{ \left| A_1 - \frac{Z}{N} \right|, \left| A_1 - \frac{Z+1}{N} \right|, \left| (1 - A_1) - \frac{N-Z}{N} \right|, \left| (1 - A_1) - \frac{N-Z-1}{N} \right| \right\}$$

The second candidate arises if we include  $p_i$  inside  $A_1$ . The third and fourth candidates are due to the other (larger) disc segment, with area  $1 - A_1$ , that shares the boundary  $l(x_i, y_i)$  with  $A_1$ .

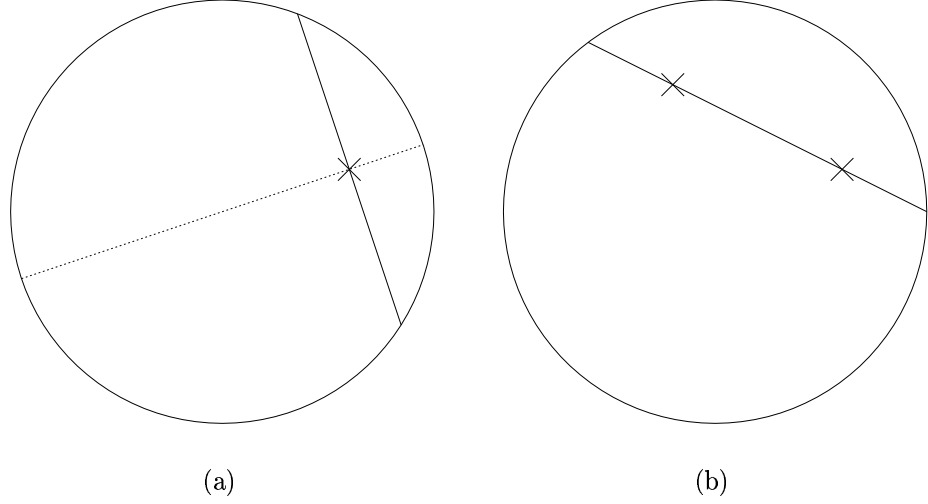


Figure 1: Half planes that would extremize the discrepancy. (a) The dotted line shows the line passing through the center of the circle and through a point  $p$ . The half-plane with its edge through  $p$  and perpendicular to the dotted line would extremizes the local discrepancy. (b) The half-plane with its edge passing through two points would also extremizes discrepancy locally.

Simplifying the third and fourth candidates shows that they are exactly the same as the first and second candidates respectively. Hence we can simplify the discrepancy  $\Delta[\mathcal{P}; A]$  to

$$\begin{aligned}
& \max \left\{ \left| A_1 - \frac{Z}{N} \right|, \left| A_1 - \frac{Z+1}{N} \right|, \left| (1-A_1) - \frac{N-Z}{N} \right|, \left| (1-A_1) - \frac{N-Z-1}{N} \right| \right\} \\
&= \max \left\{ \left| A_1 - \frac{Z}{N} \right|, \left| A_1 - \frac{Z+1}{N} \right| \right\} \\
&= \begin{cases} A_1 - \frac{Z}{N} & , \text{ if } Z < A_1 N - \frac{1}{2} \\ \frac{Z+1}{N} - A_1 & , \text{ otherwise.} \end{cases}
\end{aligned}$$

As for type (ii), there are  $2^{\binom{N}{2}}$  ways of choosing  $A$  such that it contains two points of  $P$  on its boundary. And for each  $A$ , we have to check  $N-2$  points to see if they lie inside  $A$ . Hence the half plane discrepancy of a set of  $N$  points in the unit disk can be computed by brute force in  $O(N^3)$  time. The details for calculating  $\Delta[\mathcal{P}; A]$  for type (ii) disc segments are very similar as that for type (i) and shall not be repeated here.

Point sets with three or more collinear points can be ignored by the following argument since

we are really interested in low circular discrepancy sequences: The discrepancies of point sets with three or more collinear points can always be reduced by moving one of these points slightly so that it is now no longer collinear with the rest. By the same token, disc segments with three or more points on its boundary are very rare (and can be handled separately) when computing the discrepancy of well known sequences such as the Halton and Sobol sequences.

## 4 The vortex points

In this section, we describe a method for generating sequences with a finite number of points in  $D$  using Monte-Carlo simulations of a physical vortex gas system.

Given a finite set of  $N$  points,  $P_N$  lying on some surface, consider the functional  $E(P_N) = \sum_{ij} f(r_{ij})$  where the sum is taken over all pairs of points.  $r_{ij}$  is the separation between the  $i$ -th and  $j$ -th points. If the surface is a closed  $n$ -sphere (like points on the circumference of a circle or points on surface of the globe) and if  $f$  is monotonously decreasing on that sphere, then by symmetry arguments, the set  $P_N$  that would minimize  $E$  is one in which all the points are most spread apart. Hence we can use any arbitrary monotone function  $f$  to obtain a ‘uniformly distributed’ set of points on the closed spherical surfaces by numerically minimizing  $E$  on that surface.

To find such ‘uniformly distributed’ points inside the unit disc, we shall use the functional  $E(P_N) = \sum_{ij} f(r_{ij}) + \beta \sum_i (r_i^2)$ , where the first sum is over all pairs of points. The second sum is over all individual points and  $r_i$  is the distance of the  $i$ -th point from the origin. The second sum in  $E$  ensures that the set  $P_N$  that minimizes  $E$  would have to be bounded in size. Also since  $f$  depends only on the separation of two points, then by symmetry arguments, the minimizing set must be radially symmetric. So the minimizing set would be bounded inside a disc of radius  $R(f, \beta, N)$ . The set can then be rescaled to the unit disc by dividing the coordinates of each point by  $R$ .

However unlike the previous closed  $n$ -sphere case, an arbitrary monotone  $f$  would not cause the minimizing set to be ‘uniformly distributed’. The distribution of the minimizing set from such a function would depend on  $r$ . On the two dimensional plane when  $f$  is the log function, the minimizing set was shown in [5] to be ‘uniformly distributed’ inside a radius that has a simple dependence on  $\beta$  and  $N$ . Outside this radius, the distribution drops to zero.

This log interaction arises in the physical interaction of  $N$  point vortices of equal circulation and signature [7]. Their interaction is governed by the logarithmic Hamiltonian:

$$H_N(\vec{s}) = - \sum_{j < k}^N \ln |z_j - z_k|, \quad (1)$$

where  $z_j \in \mathcal{C}$  is the position of the  $j$ -th vortex in the complex plane.  $\vec{s}$  represents the state of the entire vortex system.

Rotational invariance of the Hamiltonian implies that the moment of vorticity:

$$\Gamma(\vec{s}) = \sum_{j=1}^N |z_j|^2$$

is a first integral of motion.

Hence the functional  $E(P_N) = - \sum_{ij} \log(r_{ij}) + \beta \sum_i (r_i^2)$  corresponds to the augmented energy of an  $N$  identical point vortex gas system.

The equilibrium distribution of point vortex gas on the plane in thermal contact with an energy reservoir is described by the partition function:

$$Z(\beta, \mu) = \int_{R^2} dz_1 \dots \int_{R^2} dz_N \exp(-\beta H) \exp(-\mu \Gamma),$$

where  $\beta$  is the inverse temperature, and  $\mu$  is the Lagrange multiplier associated with the moment of vorticity of the system.

The exact partition function remains unsolved. However, to obtain the equilibrium vortex gas distribution, a Monte-Carlo simulation of the system is carried out [2]. When the Lagrange multipliers  $\beta$  and  $\mu$  are large enough, the vortex gas distribution becomes crystalline [2]. They are regularly spaced apart in a virtual bounding circle of radius  $\sqrt{\beta N / (2\mu)}$ . We shall refer to this distribution as the regular vortex gas distribution.

Figure 2(a) shows a particular vortex distribution obtained by Monte Carlo simulations with  $\beta = 1$  and  $\mu = 2$ . Figure 2(b) shows a vortex distribution at a higher value of  $\beta = 1000$  and  $\mu = 2000$ . We are interested to find the circular discrepancy,  $\Delta[\mathcal{P}]$  of these point vortices. For this, the vortices will be scaled from the circle  $D_{R=\sqrt{\beta N / (2\mu)}}$  onto  $D$  by a uniform scaling about the origin of the system.

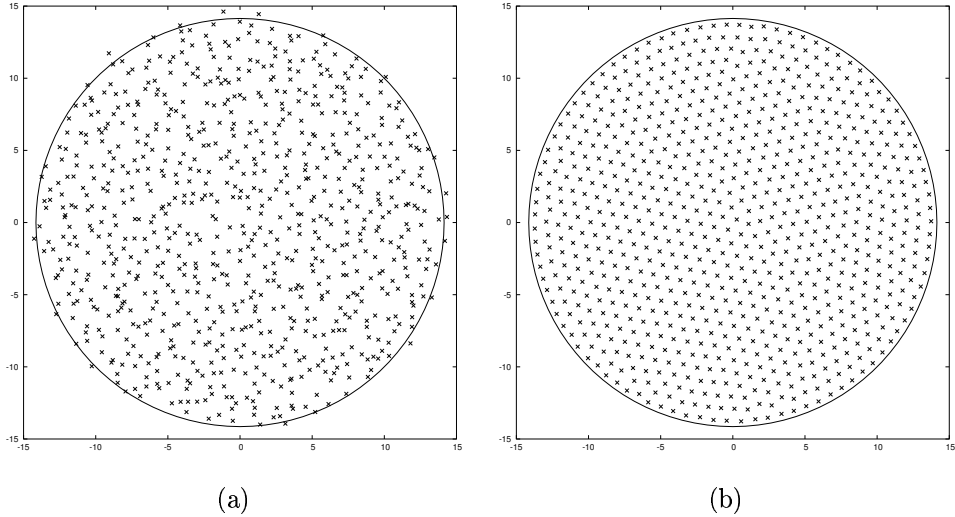


Figure 2: (a) Irregular vortex distribution of 400 vortices at  $\beta = 1, \mu = 2$ . Most of the points lies in a circle of radius 14.14. (b) Regular vortex distribution of 400 vortices at  $\beta = 1000, \mu = 2000$ . All the points are well spaced from each other and they all fall inside a circle of radius 14.14.

## 5 Other sequences

A lot of studies have been done to obtain low square discrepancy point sets on the unit square,  $I_2 = [0, 1) \times [0, 1)$ . While it is possible to define the square discrepancy using half planes (as in the circular discrepancy), we shall not do that here. The square discrepancy of point sets on  $I_2$  is more commonly defined using subintervals whose sides are parallel to the edge of  $I_2$ . Because many sequences have been developed so as to achieve a low discrepancy with respect to this definition, we shall use this definition in this paper.

*Definition:* Let  $\mathcal{P}$  be an arbitrary distribution of  $N$  points in  $I_2$ . For each subinterval  $J = (x_1, x_2) \times (y_1, y_2) \cap I_2$ , let  $Z[\mathcal{P}; J]$  denote the number of elements of  $\mathcal{P}$  which lies in  $J$ . We define the square discrepancy of  $\mathcal{P}$  with respect to  $J$  as

$$\Delta_s[\mathcal{P}; J] = \left| \frac{Z[\mathcal{P}; J]}{N} - \mu(J) \right|$$

where  $\mu(J)$  denotes the usual area of  $J$ . The square discrepancy of  $\mathcal{P}$  is then defined as

$$\Delta_s[\mathcal{P}] = \sup_J \Delta[\mathcal{P}; J]$$

where the supremum is taken over all subinterval  $J$ .

As for the circular discrepancy, we can identify a finite set of subintervals  $J$  that would have maximum local square discrepancy. Thus the square discrepancy of a sequence can also be measured in finite time.

The Hammersley sequence and the Sobol sequence are quasi-random sequences with low square discrepancy. They are generated using algorithms from number theory, rather than randomly. We shall map them onto  $D$  and then measure the corresponding circular discrepancy. To obtain a sequence in  $D$  from a sequence in  $I_2$ , we first need a suitable mapping between these two areas.

## 5.1 Mapping the square to a disc.

We shall use two different ways of obtaining a sequence in  $D$  from one on  $I_2$ .

Method 1: Let  $p$  be a point in the unit square with Cartesian coordinates  $(x, y)$ . We map it the point  $p^*$  on the disc of unit area  $D$ , where  $p^*$  has the polar coordinates  $(\sqrt{(x/\pi)}, 2\pi y)$ .

Remark: Under this mapping, an area element  $dx dy$  in the unit square maps to an area of the same measure on  $D$ .

Proof: On  $D$  the area element is  $r dr d\theta$ . Using  $dr = dx/(2\sqrt{\pi x})$  and  $d\theta = 2\pi dy$ , we get the area element  $r dr d\theta = dx dy$ . •

A second method of obtaining points in  $D$  from a distribution is as follows. We shall pick only those points that lies in the circle inscribed in  $I_2$ . Points outside this circle will be discarded. We make this precise with the following definition.

Method 2: Let  $\mathcal{P}$  be a distribution of  $N$  points in the unit square. Then  $\mathcal{P}^* = \{(x, y) \in \mathcal{P} : (x - 1/2)^2 + (y - 1/2)^2 \leq 1/4\}$  would be a distribution of  $N^* \leq N$  points in the disc of radius  $1/2$ . The distribution  $\{(2(x - 1/2)/\sqrt{\pi}, 2(y - 1/2)/\sqrt{\pi}) : (x, y) \in \mathcal{P}^*\}$  then consist of  $N^*$  points in  $D$ .

We shall see in section 6.2, that  $\Delta_s[P_1] < \Delta_s[P_2]$  does not imply  $\Delta[P_1] < \Delta[P_2]$ .

Figures 4, 5 and 6 shows three transformations from the  $I_2$  to  $D$  using method 1. Figures 7, 8 9 shows three mappings from  $D$  to the  $I_2$  also using method 1. In figure 9(a), we obtained a distribution of 400 points in  $D$  by method 2 on 1024 points of the Hammersley sequence on  $I_2$ .

## 5.2 Hammersley Sequence

The Hammersley point set for a two dimensional point  $x_n$  is defined as [9]:

$$x_n = \left( \frac{n}{N}, \phi_2(n) \right) \text{ for } n = 0, 1, \dots, N - 1,$$

where  $\phi_2(n)$  is the base two radical inverse function. The base two radical inverse function for an integer  $n$  is given by:

$$\begin{aligned} \text{If } n &= a_0 2^0 + a_1 2^1 + \dots + a_m 2^m, \text{ where } a_i = 0 \text{ or } 1, \\ \text{then } \phi_2(n) &= a_0 2^{-1} + a_1 2^{-2} + \dots + a_m 2^{-(m+1)} \end{aligned}$$

## 5.3 Antonov-Saleev variant of the Sobol sequence

The Sobol sequence generates numbers between zero and one directly as binary fractions of length  $w$  bits from a set of special binary fractions,  $v_i$ ,  $i = 1, 2, \dots, w$ , called *direction numbers*. We shall not go into the generation of  $v_i$  except to say that it is obtained recursively from the coefficients of an arbitrary primitive polynomial in the field  $Z_2$  [4, 12].

With the direction numbers, the Antonov-Saleev variant of the Sobol sequence for a two dimensional point  $x_n = (x_n^1, x_n^2)$  for  $n = 1, 2, \dots, m$  is obtained by [1]:

$$x_n^i = g_1^n v_1^i \oplus g_2^n v_2^i \oplus \dots \text{ for } i = 1, 2 \tag{2}$$

where  $G(n) = \dots g_3^n g_2^n g_1^n$  is the Gray code binary representation of  $n$ . Here  $\oplus$  denotes the bitwise XOR operator.

### 5.3.1 Example

Suppose in the first dimension we have  $v_1^1 = 0.1$ ,  $v_2^1 = 0.11$  and  $v_3^1 = 0.111$ . The Gray code binary representation  $G(n)$ , for  $n$  up to six is:

$$\begin{aligned} G(1) &= 1 \oplus 0 = 1 \\ G(2) &= 10 \oplus 01 = 11 \\ G(3) &= 11 \oplus 01 = 10 \end{aligned}$$

$$G(4) = 100 \oplus 010 = 110$$

$$G(5) = 101 \oplus 010 = 111$$

$$G(6) = 110 \oplus 011 = 101$$

To compute  $x_6^1$ , we first note from  $G(6)$  that  $g_1^6 = 1, g_2^6 = 0$  and  $g_3^6 = 1$ . Then from equation 2 we have,

$$\begin{aligned} x_6^1 &= v_1^1 \oplus v_3^1 \\ &= 0.100 \oplus 0.111 \\ &= 0.011 \end{aligned}$$

In practice, we would calculate  $x_n^1$  more efficiently using an equivalent recursive algorithm [4]:

$$x_{n+1}^1 = x_n^1 \oplus v_c^1 \tag{3}$$

where  $c$  is the position of the right-most zero bit in the binary representation of  $n$  (adding a leading zero to  $n$  if necessary), and  $x_0^1 = 0$ . With this algorithm we find the first six non-zero term of  $x_i^1$ :

$$\begin{aligned} x_0^1 &= 0, c = 1; \\ x_{01}^1 &= x_0^1 \oplus v_1^1 = 0.0 \oplus 0.1 = 0.1, c = 2; \\ x_{10}^1 &= x_{01}^1 \oplus v_2^1 = 0.10 \oplus 0.11 = 0.01, c = 1; \\ x_{011}^1 &= x_{10}^1 \oplus v_1^1 = 0.01 \oplus 0.10 = 0.11, c = 3; \\ x_{100}^1 &= x_{011}^1 \oplus v_3^1 = 0.110 \oplus 0.111 = 0.001, c = 1; \\ x_{101}^1 &= x_{100}^1 \oplus v_1^1 = 0.001 \oplus 0.100 = 0.101, c = 2; \\ x_{110}^1 &= x_{101}^1 \oplus v_2^1 = 0.101 \oplus 0.110 = 0.011, c = 1. \end{aligned}$$

The values for the second dimension  $x_i^2$  are computed in a similar manner by using a different set of direction numbers  $v_i^2$ . The implementation of the Antonov-Saleev variant of the Sobol sequence used in this paper was obtained from [11].

## 6 Comparison of discrepancies

In the two subsections below, we will present numerical results on the discrepancy of the vortex sequence generated by the above Monte Carlo code. A simple algorithm for computing the discrepancies of finite sequences will be introduced based on the theoretical results discussed earlier.

### 6.1 Algorithm for computing discrepancy

In the algorithm below  $p[1], p[2] \dots p[N]$  are  $N$  points in the set  $\mathcal{P}$ .  $D(p[i])$  and  $D(p[i], p[j])$  are sub-functions to calculate the discrepancy when the half-plane passes through  $p[i]$  or both  $p[i]$  and  $p[j]$ . These sub-functions were discussed in section 3.

```
Find_Circular_Discrepancy( P )
{
    discrepancy = 0;

    \\ Find the discrepancy of a half-plane that passes
    \\ through one point, p[i] of P.
    for ( each point: p[i] )
        discrepancy = max ( discrepancy, D( p[i] ) );

    \\ Find the discrepancy of a half-plane that passes
    \\ through two points p[i] and p[j] of P.
    if ( N > 1 )
    {
        for ( each pair: p[i], p[j] )
            discrepancy = max ( discrepancy, D( p[i], p[j] ) );
    }
    return discrepancy;
}
```

## 6.2 Numerical results 1

Table 1 shows the discrepancy values for the sequences in figures 4 to 9. All these sequences has  $N = 400$ . An explanation on how each sequence are generated are given as captions following each figure.

	Square Discrepancy	Circular Discrepancy
Fig 4: Uniform	0.0975	0.05
Fig 5: Hammersley 1	0.0136035	0.0169734
Fig 6: Sobol	0.0182048	0.021981
Fig 7: Vortex regular ( $\beta = 1000, \mu = 2000$ )	0.126578	0.0176981
Fig 8: Vortex irregular ( $\beta = 1, \mu = 2$ )	0.0467964	0.0248931
Fig 9: Hammersley 2	0.051529	0.0242217

Table 1: Discrepancies of the 400 points in figures 4 to 9.

Clearly, a sequence with low square discrepancy need not have a low circular discrepancy and vice-versa. In particular, the ‘regular vortex’ distribution has the highest square discrepancy,  $\Delta_s[\mathcal{P}]$ , however its circular discrepancy  $\Delta[\mathcal{P}]$  is second lowest after the ‘Hammersley 1’ distribution.

## 6.3 Numerical results 2

Here, we look at the behavior of circular discrepancy with  $N$ .

Figure 3 shows the circular discrepancy for the regular vortex sequence, the Sobol sequence and the Hammersley sequence for  $N$  up to 3400. The data points for the ‘regular vortex’ are obtained using  $\beta = 2000$  and  $\mu = 1000$ . The distribution for the ‘Hammersley sequence’ and ‘Sobol sequence’ are obtained by applying the transformation (method 1) in section 5.1 to the respective sequence on the square.

The general trend is that the discrepancy decreases with more points. However this is not always the case.

For almost all  $N$ , the ‘regular vortex’ distribution has the lowest circular discrepancy among the three sequences, with the Hammersley sequence coming closest to it.

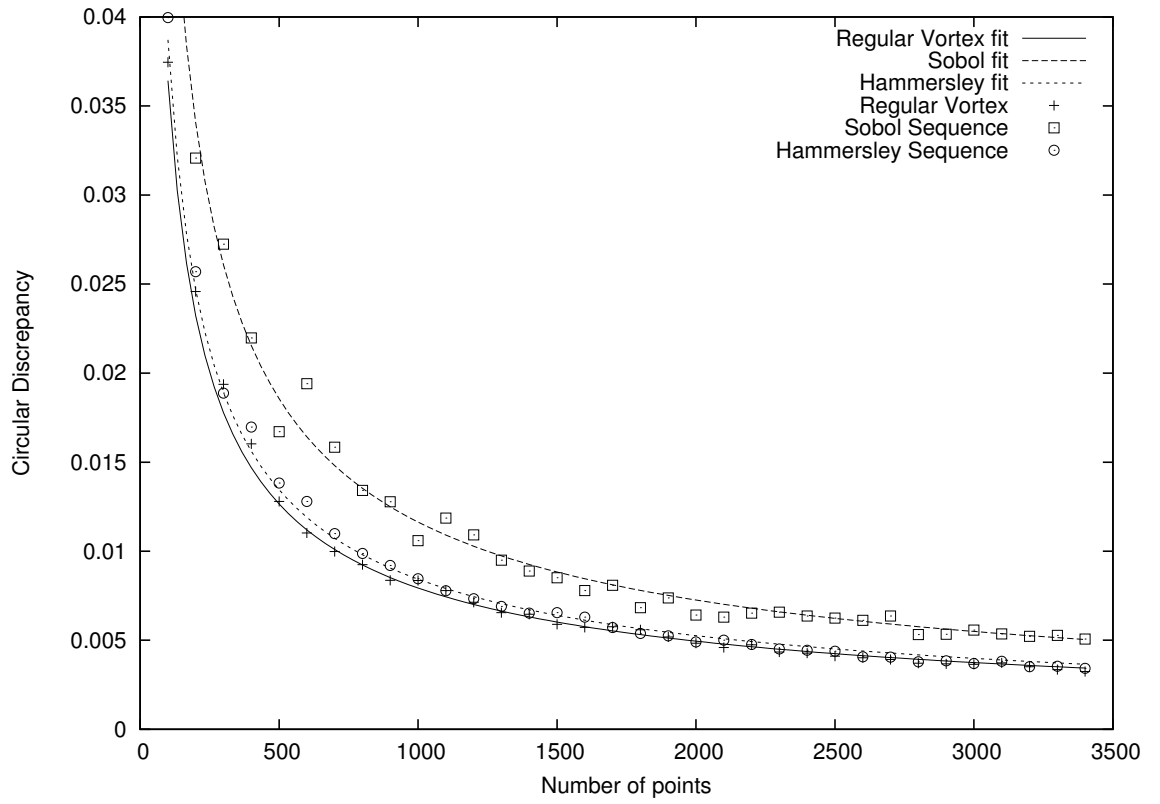


Figure 3: Graph of circular discrepancy with the number of points. The data points greater than  $N = 500$  are fitted to the function  $f(x) = cN^{-3/4}(\log N)^{1/2}$ .

The data points greater than  $N = 500$  are fitted to the function  $f(x) = cN^{-3/4}(\log N)^{1/2}$  where  $c$  is a constant, using the least square fit. The constants  $c$  for each sequence are given in table 2.

Sequence	$c$
Vortex regular ( $\beta = 2000, \mu = 1000$ )	0.536733
Sobol	0.787307
Hammersley	0.576499

Table 2: The constant for the least square fit to  $f(x)$ .

## 7 Conclusion

The equilibrium vortex gas distribution at high  $\beta$  and  $\mu$  can be used to provide a convenient low circular discrepancy point set. These point sets would be useful if one wishes to sample a fixed number of data on a circular domain.

These methods can be generalized to higher dimensions,  $d > 2$ , by modifying the Hamiltonian in equation 1 to:

$$H_N(\vec{s}) = \sum_{j < k}^N \frac{1}{|z_j - z_k|^{4-d}}.$$

The expression for the moment of vorticity and the partition function remains unchanged. At high  $\beta$  and  $\mu$ , one would obtain a regular distribution of  $N$  points in the hyper-sphere of radius  $\sqrt[d]{(d-2)\beta N/(2\mu)}$ .

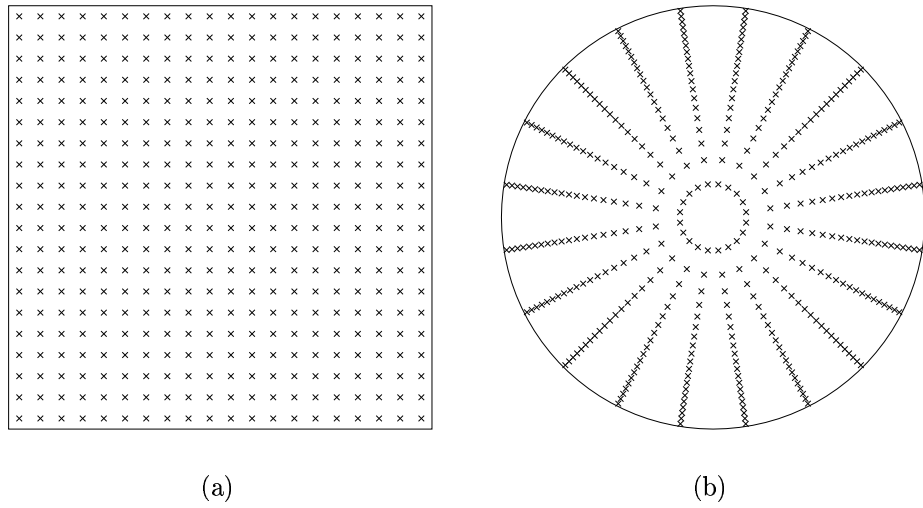


Figure 4: (a) Uniform distribution of 400 points in  $I^2$ . (b) Using the transformation in method 1 of section 5.1, the distribution becomes rays on a disc.

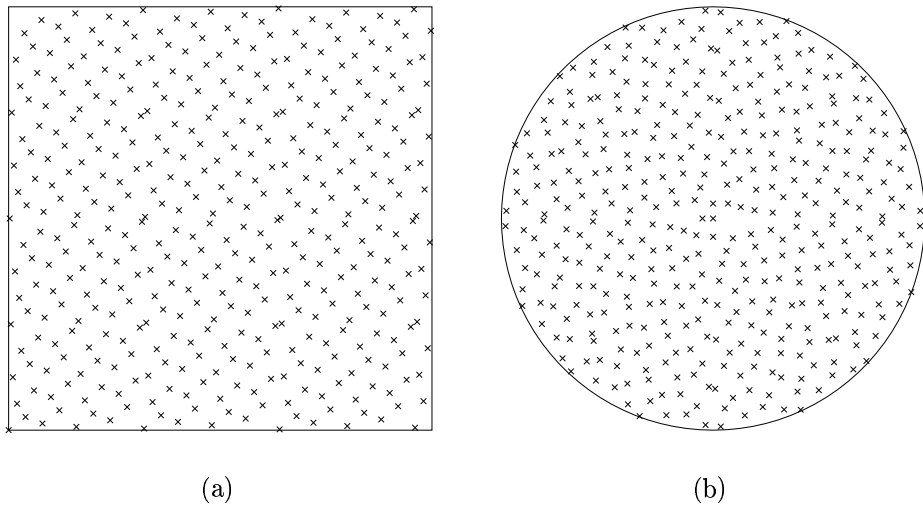


Figure 5: (a) 400 points from the Hammersley sequence. (b) Transformation of the Hammersley sequence onto the disc using method 1 of section 5.1.

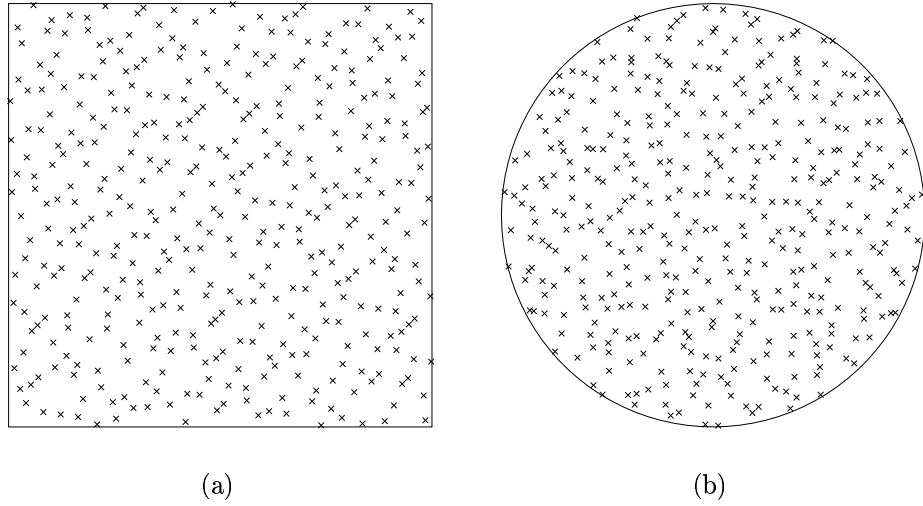


Figure 6: (a) 400 points from the Antonov-Saleev variant of the Sobol sequence. (b) Transformation of the Antonov-Saleev variant of the Sobol sequence onto the disc using method 1 of section 5.1.

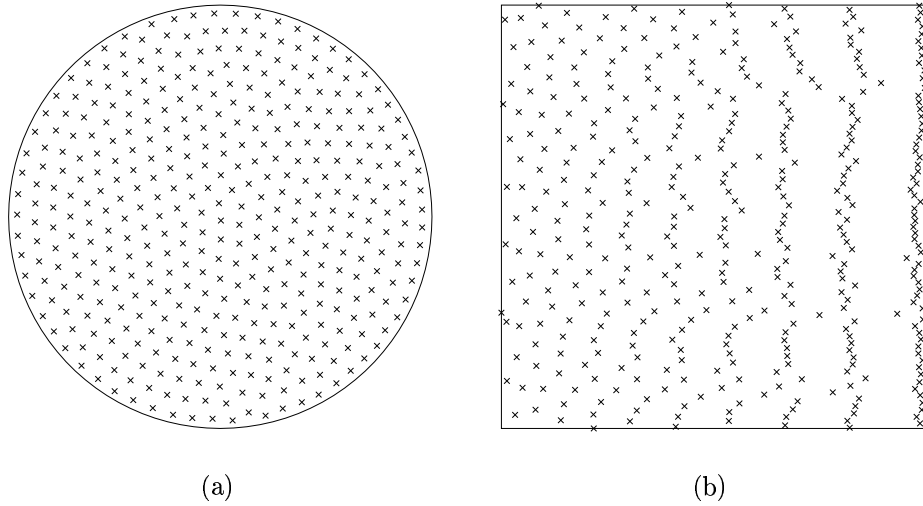


Figure 7: (a) A regular vortex distribution of 400 points from a particle Monte Carlo simulations at  $\beta = 1000$  and  $\mu = 2000$ . The boundary of the sequence is set to be  $\sqrt{\beta N / (2\mu)}$ . (b) The regular vortex distribution is mapped onto  $I_2$  using method 1 of section 5.1.

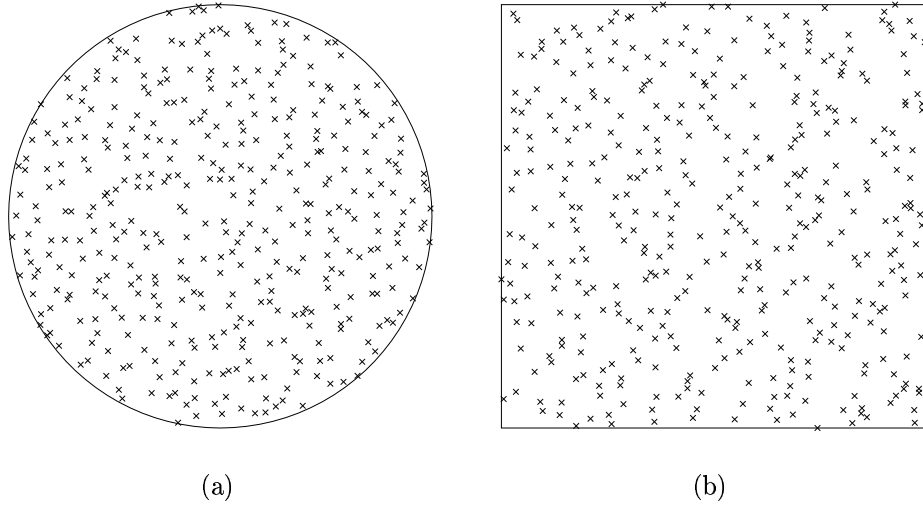


Figure 8: (a) Irregular vortex distribution of 400 points obtained by taking the closest 400 points from the center of a particle Monte Carlo simulation with 800 particles ran at  $\beta = 1$  and  $\mu = 2$ . The boundary is chosen to be half the sum of the distance of the 400th particle and 401st particle. (b) The irregular vortex distribution is mapped onto  $I_2$  using method 1 of section 5.1.

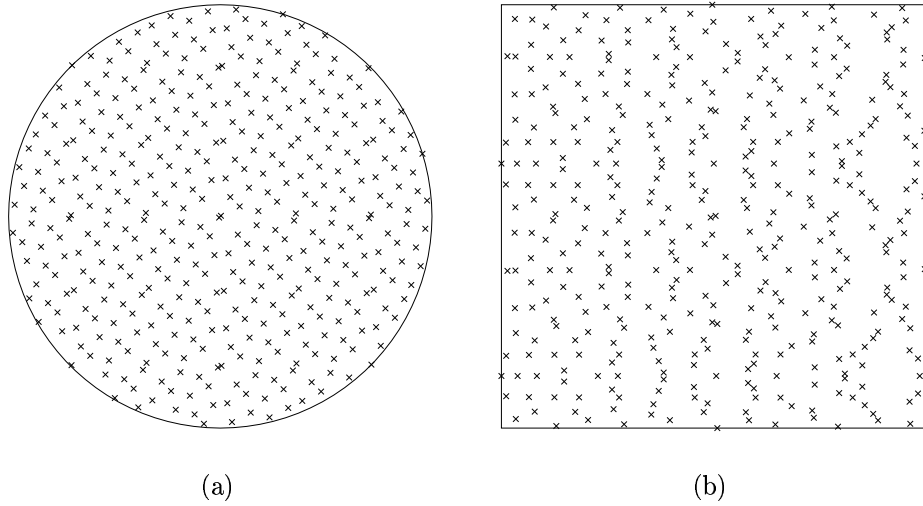


Figure 9: (a) The first 400 points closest to the center obtained from the Hammersley sequence of 1024 points. The boundary of the sequence is chosen at halfway between the 400th and 401st point. (b) The Hammersley sequence is mapped onto  $I_2$  using method 1 of section 5.1.

## References

- [1] I. A. Antonov and V. M. Saleev, *An economic method of computing LP-sequences*, USSR Computational Mathematics and Mathematical Physics **19** (1979), 252–256.
- [2] Syed M. Assad and Chjan C. Lim, *Statistical equilibrium of the Coulomb / vortex gas on the unbounded 2-dimensional plane*, Discrete and Continuous Dynamical Systems-Series B (2003), In press.
- [3] J. Beck and W. W. L. Chen, *Irregularities of distribution*, Cambridge University Press, 1987.
- [4] Paul Bratley and Bennett L. Fox, *Algorithm 659 implementing Sobol's quasirandom sequence generator*, ACM Transactions on Mathematical Software **14** (1988), no. 1, 88–100.
- [5] Chjan C. Lim and Syed M. Assad, *A variational principle for the statistical equilibrium of single-species vortex gas and cylindrical electron plasmas*, In preparation.
- [6] William J. Morokoff and Russel E. Caflisch, *Quasi-Monte Carlo Integration*, Journal of Computational Physics **122** (1995), no. 2, pp. 218–230.
- [7] Paul K. Newton, *The N-vortex problem: Analytical techniques*, Springer-Verlag New York, 2000.
- [8] H. Niederreiter, *Quasi-Monte Carlo methods and pseudo-random numbers*, Bulletin of the Mathematical Society **84** (1978), no. 6, 957–1041.
- [9] H. Niederreiter, *Construction of low-discrepancy point sets and sequences*, Sets, Graphs and Numbers (Budapest), vol. 60, 1991, pp. 529–559.
- [10] Art B. Owen, *Monte Carlo extension of quasi-Monte Carlo*, Proceedings of the 1998 Winter Simulation Conference, 1991, pp. 571–577.
- [11] W. H. Press, S. A. Teukolsky, W. T. Vetterling, and B .P. Flannery, *Numerical recipes in C: The art of scientific computing*, Cambridge University Press, 1992.
- [12] I. M. Sobol, *On the distribution of points in a cube and the approximate evaluation of integrals*, USSR Computational Mathematics and Mathematical Physics **16** (1976), 236–242.